Available online at www.sciencedirect.com

ScienceDirect

Procedia Structural Integrity 47 (2023) 102–112

Structural Integrity Procedia

www.elsevier.com/locate/procedia

27th International Conference on Fracture and Structural Integrity (IGF27)

Wrinkling of soft bilayers created with additive manufacturing: Experimental tests, finite element modelling and analytical validation.

Ranim Hamaied[a,b]*, Chao Gao[a], Andrea Spagnoli[b], Filippo Berto[c], Chiara Bertolin[a]

[a]*Norwegian University of Science and Technology (NTNU), Depatement of Mechanical and Industrial Engineering, Trondheim, Norway*
[b]*University of Parma, Department of Engeneering and Architecture, Parma, Italy*
[c]*La Sapienza University of Rome, Department of Chemical Engineering, materials and Environment, Rome, Italy*

Abstract

In the leather manufacturing industry, the necessity to introduce new leather-surrogate materials is motivated by the huge environmental footprint of the leather production process. In fact, tanning requires a lot of resources, like water and energy, but also chemicals that can be harmful to the environment and the workers as well. The contribution focuses on how the mechanical characteristics of materials used to imitate leatherlike membranes can be characterised using the wrinkles caused by compressive forces. TPU and PLA, two polymeric materials frequently used in 3D printing based on FDM, are here used to simulate the grain and corium layers of the hide to recreate the skin's structure. A compressive characterization of PLA material is performed. In this work, the scientific literature on wrinkling phenomenon has been revised. Wrinkling might form on leather-like soft membranes or in thin layers supported by a substrate when exposed to compressive loading. Results of critical wavelengths determined by the analytical approach using both inputs from experiments and literature, have been finally compared to various combinations of finite element models (FEM) to provide a variety of outcomes and to certify the accuracy of the study. In conclusion, this study provides a preliminary insight regarding the characterization of a 3D-printed, bi-layered material exposed to the wrinkling phenomenon that occurs every day on leather-based products.

Keywords: Additive Manufacturing; wrinkling; bilayer material; TPU; PLA; soft membrane; leather-like material; sustainability.

* Corresponding author.
E-mail address: ranim.hamaied@studenti.unipr.it

10.1016/j.prostr.2023.06.046

1. Introduction

A common phenomenon that occurs to leather is the wrinkling behaviour that can be triggered by a compressive force. To better understand this problem a large literature exists focusing on surface instabilities of compressed thin film rested on a thick substrate. Such instabilities are widespread in nature. For instance, it can be observed in leaves and flowers (Li et al. (2012)), but also on human organs like skin, brain, and airways (Cao et al. (2012); Limbert (2017); Bakiler et al. (2022)). Although, wrinkles are known to be a phenomenon that contributes to the decay of goods new application in the medical and electronical field proves that these instabilities can help to complete several tasks (Zhang et al. (2019)).

The knowledge gathered can contribute to a development of the leather industry by substituting the leather with bilayer material that resembles the behavior and mechanical properties of tanned rawhides to reduce the footprint of this huge industry. The leather structure can be approximated as bilayer system, where the grain and Corium (Haines et al. (1975)), the main layers that define the top grain, are resembled by the film and substrate.

The instability that can occur depends on the nature of the load, compression (Dillard et al. (2018)), growth (Evans et al. (2017)), film and substrate mismatching in the mechanical properties, (Genzer, J, Groenewold (2006)) and stretching of the substrate (Cao et al. (2012)). All of these can be the main causes for the formation of wrinkles.

A simple approach to predict the formation of wrinkles and the related wavelength is analysed by the work of Genzer, J, Groenewold (2006) and Cerda and Mahadevan (2003) that correlates the mechanical properties of the two materials and the geometry of the membrane with the formation of wrinkles in a bilayer system. In this work, some considerations are made on comparing the analytical method with the studies conducted by Biot (1961) that investigated the formation of wrinkles under in-plane compression using the Winkler's foundation theory.

New technologies such as additive manufacturing (AM) which gradually became a popular mean to produce specimens or goods for the industrial production and academic use in the field of soft robotic, biomedical engineering (Zhan et al. (2022)) and fashion industry (Mogas-Soldevila et al. (2020)) can nowadays be implemented to speed the production process, reduce the resources employed, and improve the quality control of the finale product.

We present here a bilayer system where the film is composed by Polylactic Acid (PLA) and the substrate with Thermoplastic polyurethane (TPU), both the materials are widely used in AM and present a good bonding. A compressive characterization of the PLA is performed following the ASTM D695 to obtain the values for the compressive strength and Young's Modulus.

In this paper, we will compare the analytical approach presented by Genzer, J, Groenewold (2006) with a numerical simulation to validate the theoretical effort toward understanding the wrinkling phenomenon incurred by compressive forces.

2. Case of study

Leather is a durable and flexible material created by tanning animal rawhides and it can be used for many products. Ensuring that this material can endure an aggressive environment who contributes to its wear and tear is a standard requirement by the leather industry. Therefore, a material that can withstand the natural decay is the key for a valid and sustainable substitute of leather.

Rawhides can be described as a soft collagenous connective tissue. Where collagen is a type of structural protein found in animals, that makes up the structure of the cells and tissue (Nezwek et al. (2022)). After the tanning process, the fibrous protein maintains its shape – three-dimensional fibrous wave - and it is known to be the solid constituent of the skin. Moreover, the dimensions of those fibers allow the distinction between the leather's layers.

Mammalian skin like those of cattle, sheep, and goat have a similar skin structure that can be divided in three layers as reported in Figure 1a. The region where the hairs are located, known as grain (A); and just underneath where the hairs roots are, the Corium (B); and finally, the flesh (C) that is the inner region defining the limit layer of the hide forming a boundary between the skin and the muscle of the animal (Haines et al. (1974)). As shown in Fig. 1b the fibrous protein collagen changes in dimension and orientation at different level within the hide. The corium (B) has the largest collagen fibers while the flesh surface (C) has thinner fibers that run in a horizontal plane. Each region described shows different mechanical properties that make leather a unique material. Therefore, a leather substitute should ideally have its same properties or better ones.

The tanning process has an additional stage where leather is divided in several thinner layers to obtain sections of the skin that have different quality. This process is called “leather splitting”. The outcome of this production phase led to three layers classified as grain split (or top grain), middle split (if the hide is thick enough) and the flesh split. The top grain is considered the more valuable section of the skin. In fact, this layer is composed of a grain that has a compact appearance and thinner collagen fibers and a part of the corium that is characterized by big fibers.

This contribution will study the wrinkling phenomenon in a soft membrane produced artificially with additive manufacturing. To this scope a simplified model of the top grain leather split with a two-layer membrane will be adopted. In such model, the grain is substituted with a thin layer called film and the corium with a thicker layer termed substrate as reported in the left side of Figure 1a.

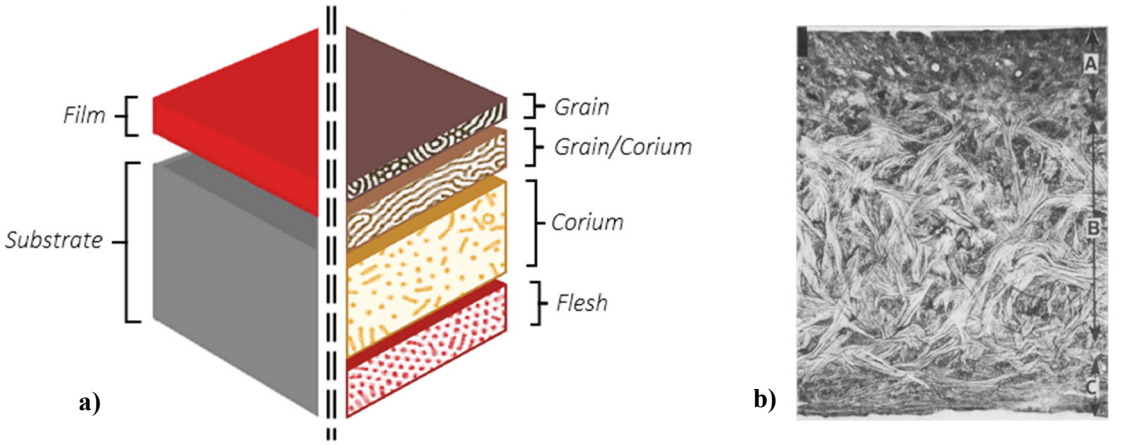

Fig. 1. (a) schematization of the structure of the rawhide and the two-layer system that resembles the top grain; (b) Cross section through cattle skin made into vegetable tanned sole leather, A: grain layer, B: corium, C: flesh layer (reproduced after Haines et al. (1974)).

2.1. Raw material

To choose the more suitable materials for producing a leather-like membrane with good bonding and mechanical properties like or better than leather, a literature review was carried out. The focus of the search was to learn how - in previous research works - the hide structure was recreated and tested to evaluate the physical properties of the leather substitute.

In the selection of materials to reproduce leather-like membranes, the sustainability played a key role. In fact, in different research conducted in literature, non-toxic, non-polluting, and fully recyclable means of processing and manufacturing goods within the leather industry were investigated to relive the high environmental impact of this industry (Mongas-Soldevilla et al. (2021)). Many works focused on polyurethane (PU) to create an artificial leather polymer made of polyurethane certified to be vegan. However, the drawback of PU leather is that it does not last long due to cracking and tearing that appear since this material is not flexible like tanned rawhides.

Another solution was presented by Mogas-Soldevila et al. (2021) where fashion goods were fabricated with additive manufacturing using leather-like silk protein composites directly derived from Bombyx mori silkworm cocoons, that have been used in the textiles and medical sutures. They combined this material with other chemicals to achieve and enhance some properties.

Another aspect that was considered during the literature review search was related to the geometries that in the leather-like membranes showed the occurrence of the wrinkling phenomenon. It appeared on a two-layer system comprised of a film bonded to an infinitely deep substrate when the entire membrane undergoes compression. The film-substate modules ration effected the wrinkling (Genzer and Groenewold (2006)) as further discussed in the following section.

The materials chosen for reproducing experimentally the bi-layered membrane were selected in order to be compatible with the experimental setup and the analytical models presented in literature ((Genzer and Groenewold (2006)).

On these bases, the first selected material was the Polylactic acid, also known as PLA, an environmentally friendly thermoplastic with a production process that uses less energy than conventional plastic production thus generating less greenhouse gases. In addition, PLA can be easily combined with other materials.

The second selected material for the experiment was the Thermoplastic Polyurethane or TPU, widely used in many industries for components, coatings but also for 3D printing. The production process as for the PLA may be fast and produces small quantity of waste.

3. Theoretical background

Soft materials like those studied in this work can undergo large deformation and they are especially susceptible to surface instabilities that result in the formation of wrinkles. This happens to a response to a wide range of stimulation like mechanical forces, changes in temperature, in the relative humidity, and in the PH values (Li et al. (2012)). For instance, these instabilities can be observed on the mammal skin but also on a compressed rubber (Biot (1962)). Understanding how this surface instabilities occur can lead to reconsidering the wrinkles as an advantageous phenomenon rather than as a phenomenon that takes part to the decay of goods like leather. The knowledge gathered found application in the biomedical field and in other sectors. On the other hand, wrinkles can be used to evaluate the mechanical properties linked with this surface instability.

To reproduce a simple model of a leather-like membrane, the top grain layer that rests on top of a thick corium layer has a different microstructure and height that consecutively leads to different mechanical properties. Therefore, the mismatching between the elastic properties of the grain and corium and their relative thickness is linked with the formation and physical appearance of wrinkles. A simple model that has been extensively used in literature to describe the mechanical behavior of a thin film resting on top of a soft elastic foundation (Genzer and Groenewold (2006)), has been exploited in this contribution to understand how the wrinkles are formed within the skin. In the model the leather has a film with thickness h and width w and it is strongly bonded with half-space elastic substrate (see Fig. 2). The simplifying hypothesis do not consider the shear stress between the two layers. The mechanical parameters involved are the elastic modulus and the Poisson ratio of the film (E_f, ν_f) and the substate (E_s, ν_s), while the geometrical properties are the thickness of the film and the width of the membrane that for simplification can be taken equal to unity. Plane strain condition is assumed for the bilayer. To trigger the formation of wrinkles a compressive action is applied in the direction reported in Fig. 2, specifically by applying uniform imposed displacements along the edge. The model can estimate the entity of the resulting force acting on the elastic foundation and describe the wrinkles based on the wavelength λ.

$$F = E_f \left[\left(\frac{\pi}{\lambda} \right)^2 \frac{wh^3}{3\left(1-\nu_f^2\right)} + \left(\frac{\lambda}{\pi} \right) \frac{E_s w}{4\left(1-\nu_s^2\right)E_f} \right] \tag{1}$$

λ denotes the wavelength of the surface instabilities of the film along the direction of the applied compressive force that is acting on the substrate. Once the loading is equal or bigger than the critical load F_c surface wrinkling occurs in the film. The corresponding critical wavelength λ_c can be obtained by posing the derivative of equation (1) with respect to λ equal to zero. By doing so the critical wavelength is equal to:

$$\lambda_c = 2\pi h \left[\frac{\left(1-\nu_s^2\right)E_f}{3\left(1-\nu_f^2\right)E_s} \right]^{1/3} \tag{2}$$

In equation (2) the critical wavelength of the wrinkles depends only on the mechanical properties of the material (elastic modulus and Poisson ratio) and on the thickness of the film h being independent from the applied stress and strain. It is observed that for small value of h and (E_f/E_s) the wrinkling period is very small while it increases if both h and (E_f/E_s) increase.

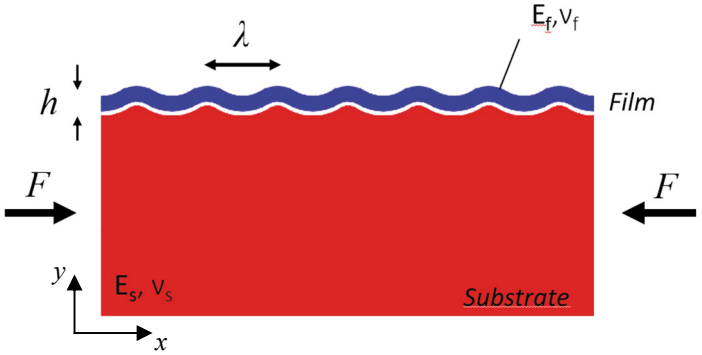

Fig. 2. Sketch of the model adopted for the analytical and numerical resolution.

Another observation can be made considering a portion of the bilayer with length λ. Assuming a sinusoidal deflection of the surface film with no debonding between the film and the substrate, interface pressures between the two layers develop. Their distribution along the interface (see eq. 3), i.e., with respect to the coordinate x, can be determined by considering the analytical solution of a frictionless contact problem available in the literature (Barber, 2018). In particular, if one takes the frictionless contact problem of a rigid sinusoidal punch pressed against an elastic half-space, the interface pressure turns out to be described by:

$$q(x) = wp(x) = \frac{2\pi E_f^* h_0 w}{\lambda} \cos^2\left(\frac{\pi x}{\lambda}\right) \tag{3}$$

$$E_i^* = \frac{E_i}{1-\nu_i^2} \qquad i = s, f \tag{4}$$

Where h_0 and w represent the dimension of the cross section of the film and lambda is the wavelength of the wrinkles that appear on the rigid surface. The total potential energy (TPE), $V(v)$, of the system (reported in eq. 5) is made up by the contribute of the flexural energy of the skin (E_s^*), the compressive deformation of the substrate, and the work produced by the compressive force F, namely:

$$V(v) = \frac{1}{2}\int_{-\lambda/2}^{\lambda/2}\left(E_s^* I\dot{v}^2 - F\dot{v}^2 + \frac{q}{h_0}v^2\right)dx \tag{5}$$

Supposing that:

$$v(x) = A\cos\left(\frac{\pi x}{\lambda}\right) \tag{6}$$

Where A is the amplitude of the wrinkling waves and the coordinate axis is such that $-\lambda/2 \leq 0 \leq +\lambda/2$. The TPE can be written as:

$$V_2(v) = \frac{1}{4} A^2 \lambda \left[E_s^* I \left(\frac{\pi}{\lambda} \right)^4 - F \left(\frac{\pi}{\lambda} \right)^2 + \frac{3}{2} \frac{\pi}{\lambda} E_f^* w \right] \tag{7}$$

The equilibrium is obtained by stationarity condition of equation (7), that is by posing the derivative of equation (7) with respect to A equals to zero. The solution obtained can be written as follows:

$$F = a\lambda^{-2} + b\lambda \tag{8}$$

The expression (8) is similar to equation (1) proposed by Genzer and Groenewold (2006) and it resembles the analysis on wrinkles made by Biot in 1962.

4. Material and methods

4.1. Sample preparation

3D printing of all the samples were performed using a bi-material printer 3ntr A4V4 (see Fig. 3a). This is a bi-material industrial printer with a printing volume of 300x171x200mm. The design of the samples was done by SSI and Full control software. After the slicing of the model was done, the design of the specimen was converted into a G-Code which gave instructions to the machine on the coordinates, speed of printing, and extrusion rate for the nozzle to print the model.

The quality of the produced printed specimens was evaluated based on the filament adherence, on the rate of extrusion (to evaluate an over or under extruded filament), and on the layers pattern sharpness. PLA specimens were all printed using the first nozzle of 0.3mm and the filament with dimension of 2.85mm. The thickness of the layer was set to 0.15 mm and the temperature, in compliance with the information given by the supplier, ranged from 200° to 210°C. The infill density was set to 100% and the carbon tray-maintained 60°C temperature, throughout the printing process. In this study the samples were all printed flat where both ends of the specimen were in contact with the carbon tray.

4.2. Compressive test specimen

To characterize the compressive mechanical behavior of the PLA, tests were carried out following the ASTM D695 standard for rigid plastic, to achieve values about the modulus of elasticity (used to define the material in the finite element simulation) and the compressive strength. To prepare the specimen so that the mechanical properties evaluated could be used to describe the behavior of a bi-layer membrane, the same load condition regarding the filament printing direction was reproduced. In fact, the direction and patterns used in the specimen could lead to a significant difference in the mechanical properties, as highlighted by Yadav et al. (2021) that did experimental tests on different specimens printed with several patterns showing how the infill design and the infill density had an impact on their compressive strength.

The printing pattern and loading condition of the specimens tested in this contribution were printed with a +/- 45° pattern to resemble the leather-like membrane.

The test specimens were designed in compliance with the regulation provided by the standards for test specimen dimensions for strength measurements. As a result, the produced specimens had a prismatic shape with a length twice its principal width (12,7*12,7*25,4 mm^3), and the specimen was rotated so that the +/- 45° layers were parallel to the printing plate. Five specimens were teste for PLA.

The machine used for the compressive test was an Instron Model 1342 (see Fig. 3b), a servo hydraulic machine with a load capacity of 100kN (the machine is in the NTNU-Norwegian University of Science and Technology Fatigue

lab). To better describe the mechanical properties five specimens were tested aligning the principal axis with the load axis and the speed of testing was set to 1,3mm/min (0,050 in./min). The displacement of the compressive disk attached to the machine was directly obtained from the measurement of the machine. The young's module was determined considering the linear part of the true stress-strain curve and the slope was estimated by a linear adjustment. The ultimate engineering stress was calculated as the relation between the maximum load reached during the test and the effective cross-section measured before the specimens were tested.

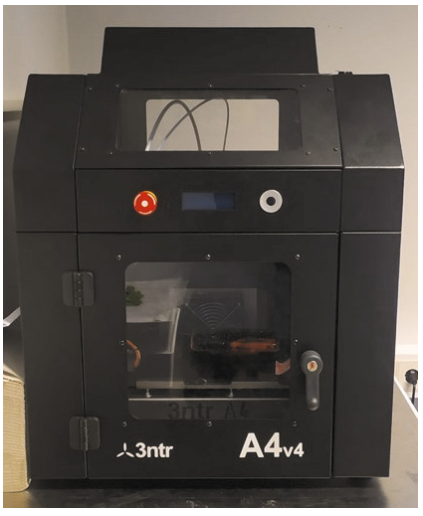

a)

b)

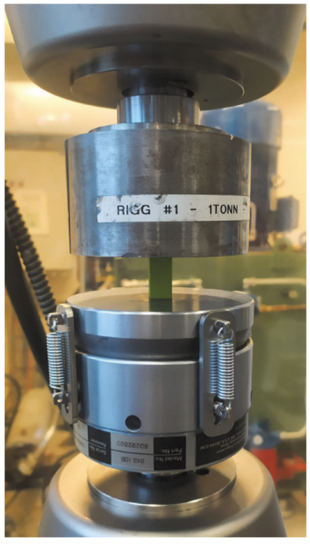

c)

Fig. 3. (a) FDM printer 3ntr A4V4; (b) Instron model 1342; (c) display of the prismatic specimen in position between the compressive plates.

4.3. Critical wavelength evaluated by the numerical simulation

For the purpose of verifying the used analytical model, a comparison was made between the analytical results and the FEM analysis. The numerical analysis was performed using Strauss7. In the analytical model the substate had the hypothesis of an infinite thickness. To reproduce this condition in the FEM analysis, the thickness of the substrate was set to a value that could reduce the elaboration time while reducing the influence of the finite substrate. To achieve this state a ratio between the thickness of the skin and the thickness of the substrate was set equal to 1/50.

A displacement of 1 mm was applied on one end of the membrane while the other end was restrained. The analyses that were performed on the model were the linear analysis, the bulking analysis, and the non-linear analysis.

5. Results

5.1. Printing outcome

The design of the five specimens was made using entirely the SSI software. This is the reason why the designed specimens as shown in the Fig. 4a have an extra volume of extruded material, raft, attached to the bottom of the prismatic shape. The results of the quality printing outcome based on the filament's adherence, extrusion rate, and pattern sharpness performed only on the prismatic printed shape are listed in the table.1. All the specimens have successfully passed the quality check. In fact, there are no filaments that easily detach from the main body, even after the compression test a good bonding can be observed on the distorted specimens. The extrusion rate was controlled throughout the printing process and there was no noticeable drastic change with the volume of material extruded. At the same time the pattern sharpness was evaluated during and after the printing process. The definition of the pattern

is clear as can be seen in the Fig. 4a where an outer border made of two filament and a +/-45° filling pattern is visible. A further evaluation was made on the surface of the prismatic specimen that was in contact with the raft. We observed that within this first layer in all the specimens, the infill density was less than 100%. To investigate better if the assigned infill density was reached after few layers or more, an extra specimen was printed. The process was suddenly interrupted about mid printing to observe if the last layer reached the desired infield density. Since this printing test did not highlight any changes in the infill density with the last printed layers, we assumed that the first layer are the only ones that may show this problem while the infill density of 100% is reached within the other layers. Fig. 4b shows all the printed specimens.

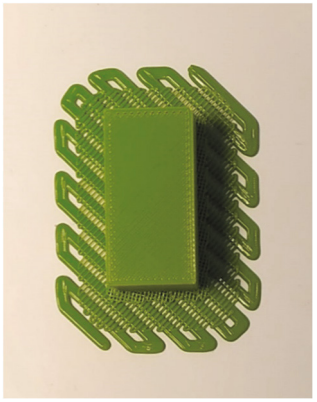

a)

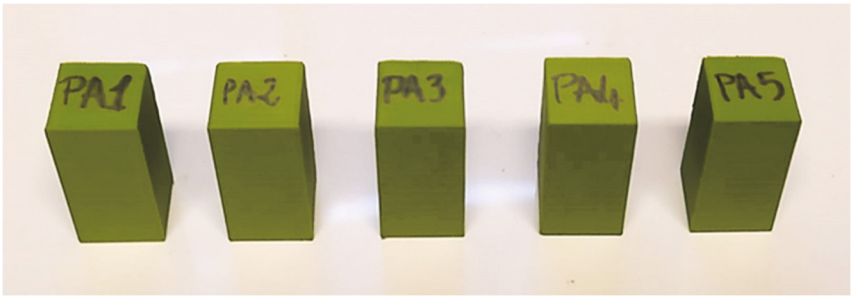

b)

Fig. 4. (a) specimen attached to the raft; (b) specimens detached from the raft.

Table 1. Quality check analysis for the specimens.

Specimen	Filament's adherence	Over/Under extrusion	Pattern sharpness
PA1	Good	Good	Good
PA2	Good	Good	Good
PA3	Good	Good	Good
PA4	Good	Good	Good
PA3	Good	Good	Good

* Good = no flaws are visible on the specimen; Bad = the specimen has some flaw

5.2. Compressive test outcome

The forces acting on the PLA specimen during the compressive test were parallel to the printing orientation. Fig. 3c shows the samples after the compression test is performed. As it can be observed, a similar deformation happened for all five PLA specimens (Fig.5), these distortions were developed mainly once the yield stress was reached. The similarity between the behavior of the specimens during the compression test is confirmed with the stress-strain curves shown in Fig. 6. the first four specimens produced the more comparable results for compressive strength while the fifth specimen had the lowest compressive strength and modulus (31.96 MPa and 1.62GPa). This behavior is attributable to a malfunction of the printing machine due the failure of the cooling system. Therefore, the fifth specimen has not be considered further in the evaluation of the average compressive strength and modulus. The curves initially exhibit a nearly linear response caused by the adjustment of the compressive disk at the initial stage of the test. After the curves are linear till the yield stress is reached. The averages of the compressive strength and young

modulus calculated from the true stress-strain curves are listed in Table 2. The compressive mechanical properties resulted not affected by the printing orientation comparing the outcomes with similar works in literature (Vukasovic et al. (2019); Prajapati et al. (2021); Ionut (2020)) This is the case outlined by Vukasovic et al. (2019) that performed compressive tests on specimens with different printing angles, showing that there isn't important dissimilarity between the results obtained for PLA specimens.

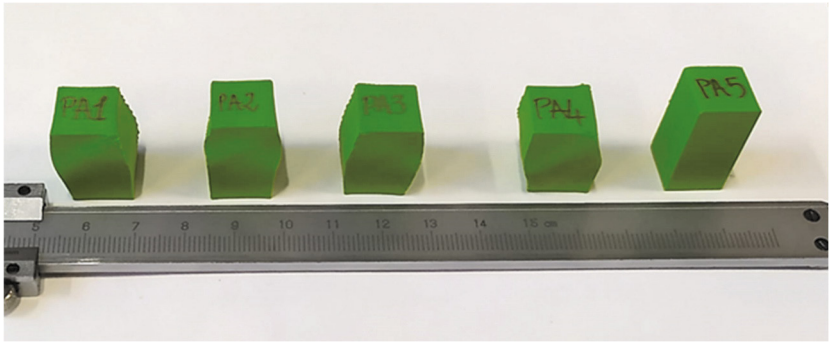

Fig. 5. Specimens after the compression test.

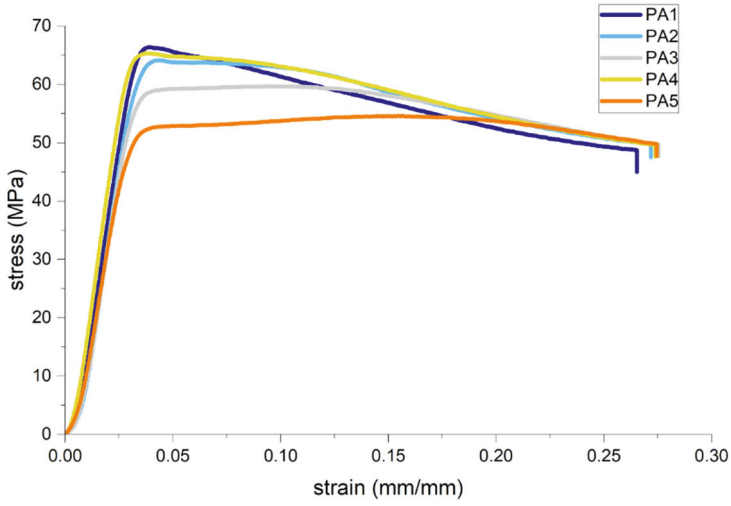

Fig. 6. True stress-strain curves for the five specimens.

Table 2. Average of the Compressive strength and the Young's Modulus for the specimens.

Specimen	Compressive strength [MPa]	Young's Modulus [GPa]
PA1	66.41	2.36
PA2	64.16	1.84
PA3	59.71	2.33
PA4	65.37	2.57
PA5*	31.96*	1.62*
Average	**63.91**	**2.28**

* These values are not considered to evaluate the average compressive strength and Young's modulus.

5.3. Model analysis: analytical and simulation results

Using the equation (2) introduced for the analytical approach to estimate the wavelength of the wrinkling instabilities, it is possible to relate the mechanical properties obtained from the compressive test with λ_c. Table 3 shows the wavelength determined for the membrane with a film thickness of 0.2 mm and a substrate thickness of 10 mm. The wavelength value was confronted using the mechanical properties evaluated by other works that performed compressive tests on PLA (Vukasovic et al. (2019); Prajapati et al. (2021); Ionut (2020)). The mechanical properties values obtained from the analytical method are comparable with those estimated in literature.

The numerical simulation performed was carried out on the same model used for the analytical approach, assuming plane stress condition. The analyses were computed with the young's module obtained from the experimental tests for PLA while for the TPU the Young's module equal to 30 MPa was considered. The Poisson ratio adopted for both PLA and TPU materials was equal to 0.45. Buckling analysis results shown in Fig. 7 outline the surface instability with a wavelength of 3.66 mm that is very similar to the wavelength evaluated with the analytical approach (i.e., 3.68 mm). To trigger the formation of wrinkles during the nonlinear analysis an imperfection was introduced for the film layer. The entity of the imperfection was similar to the results obtained from the buckling analysis reduced so that the maximum displacement was less or equal to the thickness of the film. The solution underlines the non-linearity of the wrinkle's formation on the film.

Table 3. critical wavelength evaluated with the analytical end numerical approach.

Approach adopted to estimate λ_c	λ_c [mm]
Equation 2	3.68
FEM	3.66

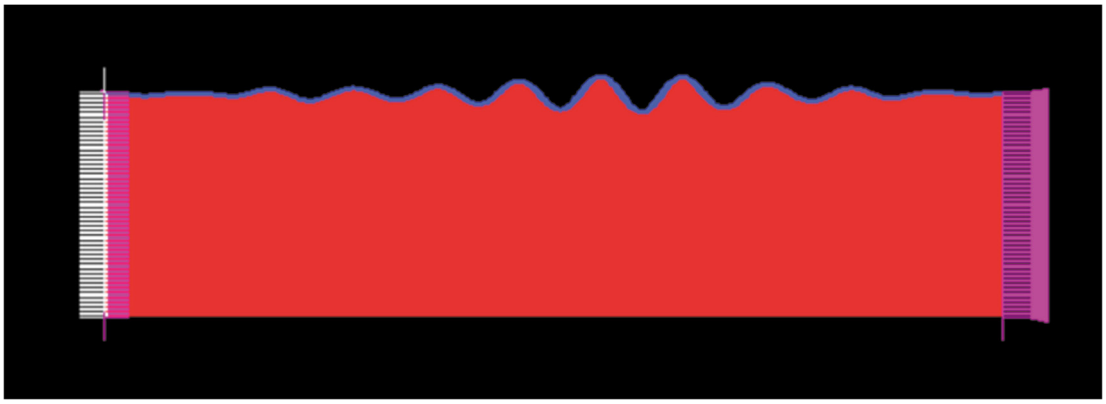

Fig. 7. Result of the buckling analysis performed on the bi-layer model; the PLA film is defined by the colour blue while the TPU used for the substrate is defined by the colour red.

6. Conclusion and future work

The aim of this work was to validate the analytical approach used to predict the formation of wrinkles within a film layer on a soft membrane resembling the leather material. Despite the difficulties encountered with the printing process for the specimen made from TPU, additive manufacturing represents a valid solution that can be implemented in the leather industry to help making the manufacturing process more sustainable in the future years (Buljan et al (2019)). I design and printing process for the PLA specimens was fast, simple, and only a small quantity of recyclable waste

was generated (i.e., the raft). Thus, FDM printing can contribute to a more sustainable mean of production minimizing water and harmful chemicals employed in the leather industry while at the same time may contribute to improving the working environment. Another important aspect regards the possibility to reduce the cruelty toward the animals engaged in the leather industry.

Both PLA and TPU are materials that can be combined to recreate a leather like membrane. Moreover, PLA is biodegradable. A more detailed study should be carried out to investigating the bonding between these two materials. In fact, since the wrinkling instabilities occurs once the critical force is reached, at that stage a debonding phenomenon could happened.

The results obtained by the numerical simulation validate the analytical approach equation (2). Moreover, the magnitude of the critical wavelength estimated for the soft membrane made of PLA and TPU is similar to the one observed on tanned rawhides by Genzer and Groenewold in 2006.

Acknowledgements

The project leading to these results has received funding from the European Union's Horizon 2020 research and innovation program (H2020-WIDESPREAD-2018, SIRAMM) under grant agreement No. 857124.

References

Li, B., Cao, Y., Feng, X., Gaoc, H., 2012. Mechanics of morphological instabilities and surface wrinkling in soft materials: a review. Soft Matter.

Cao, Y., Jiang, Y., Li, B., Feng, X., 2012. Biomechanical modelling of surface wrinkling of soft tissues with growth dependent mechanical propertires. Acta Mechanica Solida Sinica.

Limbert, G., 2017. Mathematical and computational modelling of skin biophysics: a review. The Royal society Publishing.

Bakiler, D., Javili, A., 2022. Understanding the role of interfacial mechanics on the wrinkling behavior of compressible bilayer structures under large plane deformations. Mathematics and Mechanics of Solids.

Zhang, J., Li, Y., Xing, Y., 2019. Theoretical and experimental investigations of transient thermo-mechanical analysis on flexible electronic devices. Int J Mech Sci. 160: 192–199.

Dillard, D., Mukherjee, B., Karnal, P., Batra, R., Frechette, J., 2018. A review of Winkler's foundation and its profound influence in adhesion and soft matter applicarions. Soft Matter.

Evans, A., Cheung, E., Nyberg, K., Rowat, A., 2017. Wrinkling of milk skin is mediated by evaporation. Soft Matter.

Genzer, J, Groenewold, J., 2006. Soft matter with hard skin: From skin wrinkles to templating and material characterization", Advanced Drug Delivery Reviews.

Cedra, E., Mahadevan, L., 2003. Geometry and Physicals of Wrinkling. Physical Review Letter.

Biot, M. A., 1961. Surface instability of rubber in compression. Appl. Sci. Res.

Zhan, S., Guo, A. X. Y., Cao, S. C., Liu, N., 2022. 3D Printing Soft Matters and Applications: A Review. Molecular Science.

Haines, B. M., Barlow, J. R., 1975. The anatomy of leather. journal of Material Science.

Nezwek, T., Varacallo, M., 2022. Physiology, Connective Tissue. In: StatPearls [Internet].

Haines, B. M., Barlow, J. R., 1974. Review The anatomy of leather. Materials science.

Mogos-Soldevila, L., Matzeu, G., Lo Presti, G., Omenetto, F.G., 2022. Additively manufactured leather-like silk protein materials. Material design.

Li, B., Cao, Y., Feng, X., Gao, H., 2012. Mechanics of morphological instabilities and surface wrinkling in soft materials: a review. Soft Matter.

Biot M. A., 1937. J. Appl. Mech. 4, A1–A7.

Barber, J.R., 2018. Contact Mechanicas. Solid Mechanics and its Applications.

Yadav, P., Sahai, A., Sharma, R.S., 2021. Strength and Surface Characteristics of FDM-Based 3D Printed PLA Parts for Multiple Infill Design Patterns. The Instituition of Engineers (India).

Vukasovic, T., Vivaco, J. F., Celentano, D., Garcia-Herrera, C., 2019. Characterization of the mechanical response of thermoplastic parts fabricated with 3D printing. The International Journal of Advance Manufacturing technology.

Prajapati, A. R., Rajpurohit, S. R., Patadiya, N. H., Dav, H. K., 2021. Analysis of Compressive Strength of 3D Printed PLA Part, Advances in Manufacturing Processes.

Ionut, O., 2021. PLA 3D compressive Test.

Buljan, J., Kràl', I., 2019. The framework for sustainable leather manufacture.